Influence of the Carbon Nanotube Probe Tilt Angle on the Effective Probe Stiffness and Image Quality in Tapping-Mode Atomic Force Microscopy

*Santiago D. Solares, Yuki Matsuda and William A. Goddard III**

Materials and Process Simulation Center, Division of Chemistry and Chemical Engineering, California Institute of Technology, Pasadena, California 91125

Supporting Information

1. Comparison of force curves between single-walled carbon nanotube and Si tips of comparable radius

Figure S-1 provides a comparison of the tip-sample interaction force curves obtained with a vertically aligned 30,30 single-walled carbon nanotube (SWNT) tip, of radius 1.7 nm, and a Si tip of the same radius (with side wall angles of 15º with respect to vertical). The force curve of a larger 15-nm-radius Si tip (see Figure 3 of the paper) is also provided as a reference. The result shows that the forces that emerge during imaging, and their

rate of change with respect to the tip position are of comparable magnitude for the 1.7-nm-radius tip and for the SWNT tip. The graph also shows that although the magnitudes of the forces are comparable, the curve for the Si tip is shifted to the right with respect to that of the SWNT because of its solid geometry that does not allow it to penetrate into the surface in the same way the SWNT does [recall that we modeled the substrate as a Si(100)-OH surface, whose functional groups can penetrate into the hollow center of the CNT, but not into the solid Si tip. Additionally, the SWNT walls are more susceptible to lateral deformation than the Si tip]. These force curves constitute an important result concerning the imaging of sensitive samples, because they show that if fine Si tips can be manufactured and maintained sharp during the acquisition of the images, they can also lead to reduced sample damage, as do *vertically aligned* SWNT's. This could be advantageous in environments where it is difficult to use SWNT tips, such as when the solvent is water.

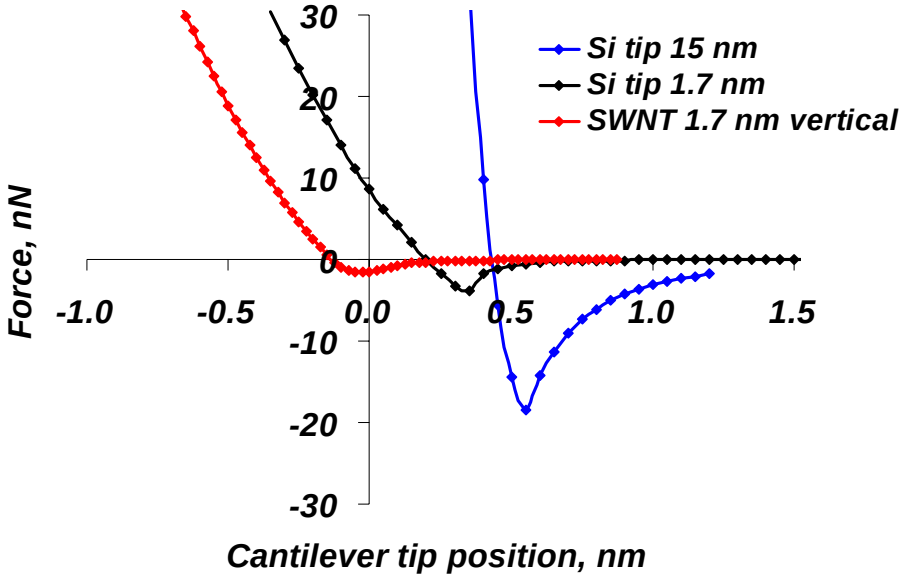

Figure S-1. Comparison of the tip-sample force curves obtained with a 30,30 single-walled carbon nanotube tip and a Si tip (both of radius 1.7 nm), and a 15-nm-radius Si tip. The graph shows that the tip-sample forces are of similar magnitude and slope for the nanotube and the 1.7-nm-radius Si tips.

2. Force curves for single-, double- and triple-walled carbon nanotube probes

Figures S-2, S-3 and S-4 show the tip-sample interaction force curves obtained for single-, double- and triple-walled carbon nanotube probes of outer diameter 3.5 nm and aspect ratio 7.5. These curves were used to calculate the terminal force gradients shown in Figure 6 of the paper. The graphs show that as the number of internal walls in the probe increases, the force curves become steeper. These curves are similar to those shown in Figure 3 of the paper, although some of them differ slightly in that they exhibit minor slippage before reaching the terminal force gradient. We attribute this to the smaller probe diameter, which makes it more susceptible to lateral bending.

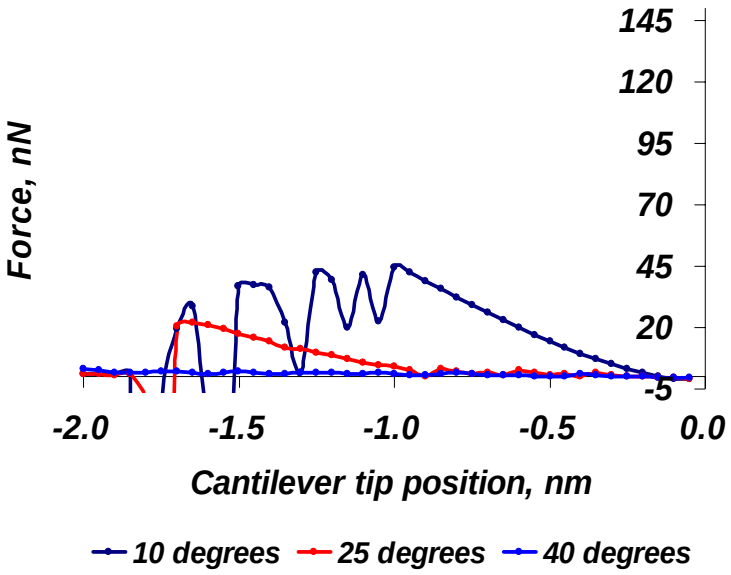

Figure S-2. Tip-sample interaction force Vs. cantilever tip position for a 25,25 single-walled carbon nanotube probe (diameter 3.5 nm and aspect ratio 7.5) imaging a Si(100)-OH surface for ϕ = 10, 25 and 40°.

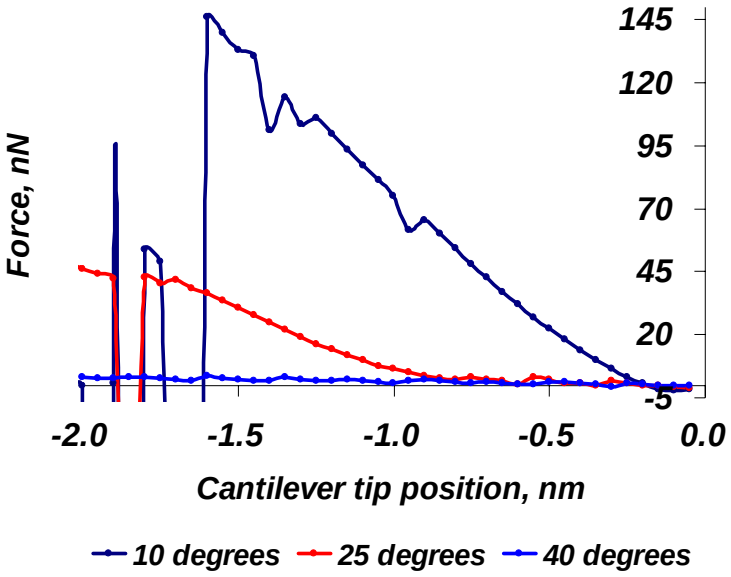

Figure S-3. Tip-sample interaction force Vs. cantilever tip position for a 25,25/20,20 double-walled carbon nanotube probe (outer diameter 3.5 nm and aspect ratio 7.5) imaging a Si(100)-OH surface for ϕ = 10, 25 and 40°.

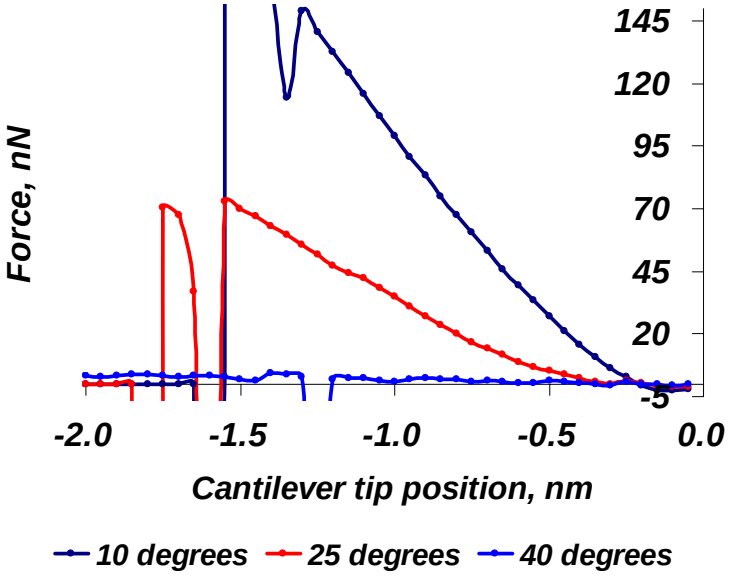

Figure S-4. Tip-sample interaction force Vs. cantilever tip position for a 25,25/20,20/15,15 triple-walled carbon nanotube probe (outer diameter 3.5 nm and aspect ratio 7.5) imaging a Si(100)-OH surface for ϕ = 10, 25 and 40°.

3. Cantilever oscillation dynamics for A_o = 20 nm

Figure S-5 illustrates the dependence of Z_{min}, F_{max} and the cantilever oscillation amplitude on the cantilever rest position for the 40,40 SWNT probe and for the Si tip imaging a Si(100)-OH surface with A_o = 20 nm. These results are qualitatively similar to those of Figure 9 of the paper (for A_o = 40 nm) but the observed variations for different values of ϕ are smaller due to the smaller excitation force amplitude. For A_o = 20 nm the oscillation amplitude and F_{max} are lower, while Z_{min} is greater than for A_o = 40 nm due to the lower excitation force and lower probe and surface deformation.

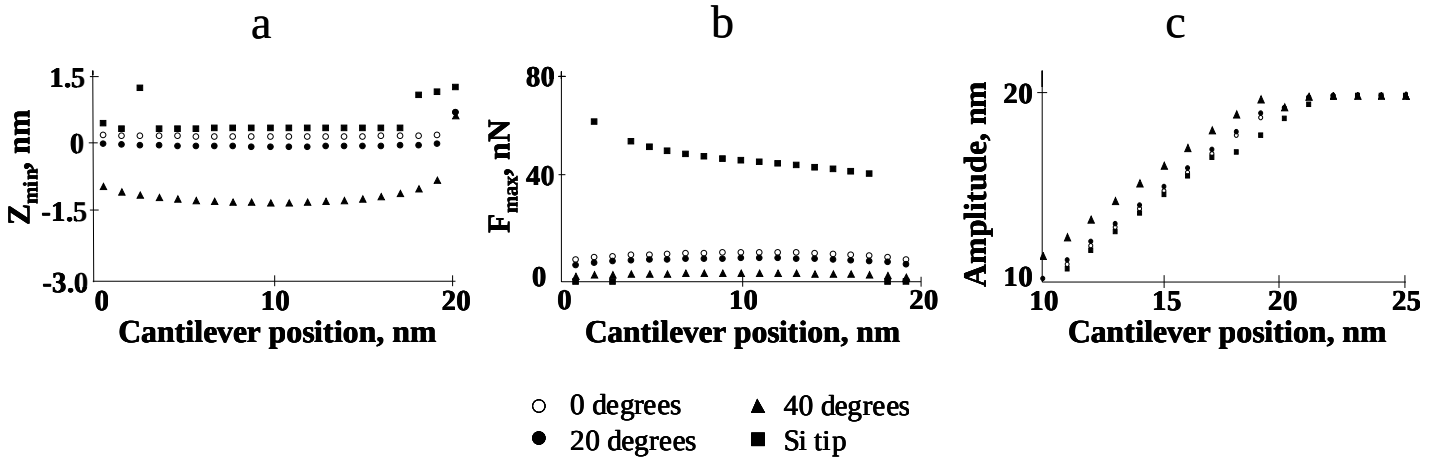

Figure S-5. Lowest cantilever position (a) and maximum tip sample force (b) observed *during one full oscillation of the AFM cantilever,* and oscillation amplitude (c) vs. cantilever rest position, for the 40,40 SWNT probe shown in Figure 1 of the paper (for ϕ = 0, 20 and 40º) and for a 15-nm radius Si tip imaging a clean Si(100)-OH surface. A_o = 20 nm in all cases. The discontinuities on the curves (such as the jump in the Z_{min} curve for the Si tip –black squares– between cantilever positions of 17 and 18 nm) correspond to the well-known transitions between the attractive and repulsive imaging regimes of tapping-mode AFM. [1] [Note that Z_{min} = 0 corresponds to the AFM cantilever rest position for which the tip (SWNT or Si) is *first* able to contact the surface].

4. Analysis of tip deformation modes

Our molecular simulation results show that the primary modes of CNT tip deformation (for the systems considered) are macroscopic bending/shearing and local deformation at the end of the tip (especially for SWNT's which have softer lateral deformation modes). They also show that local deformation can in some cases represent the main contribution to the strain energy, especially at large tilt angles. This is illustrated in Table S-1, which provides the percentage of the total strain energy in the probe (i.e. not considering the surface) that is stored in the 4 nm (10% of the total probe length) closest to the surface. These results correspond to the 40,40 SWNT probe interacting with a bare Si(100)-OH surface at a cantilever tip position of -0.5 nm (See Figure 3 of the paper). The percentages range from ~20% to 64%, indicating that local deformation is indeed significant. This is also evident in Figure S-6, which depicts the macroscopic and local deformation of the same probe for $\phi = 10^{o}$ and $\phi = 20^{o}$. Figure S-7 shows that the deformation modes can be even more complex when a sample is present. In these cases, in addition to significant local deformation, bending can occur in more than one Cartesian direction simultaneously. Due to these complex deformation modes, a classical uniform-beam analysis of tip deformation [2,3] should only be used to estimate general trends.

Table S-1. Ratio of strain energy stored in the distal 10% portion of the 40,40 SWNT probe (diameter 5.5 nm and aspect ratio 7.5) to the total strain energy, as a function of the tilt angle. These results correspond to a cantilever tip position of -0.5 nm with respect to the Si(100)-OH surface (see Figure 3 of the paper).

ϕ	**Local Strain/Total Strain**
0	0.20
10	0.26
20	0.64

30	0.60
40	0.43

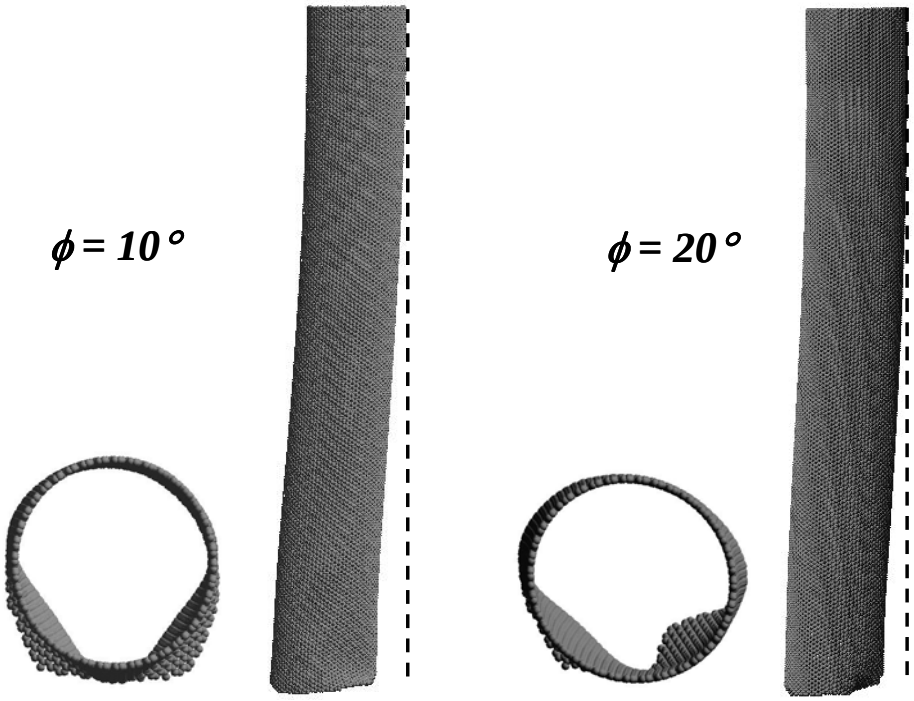

Figure S-6. Illustration of the macroscopic bending/shearing and local end-tip deformation modes for $\phi = 10^{o}$ and $\phi = 20^{o}$ (note that the probe images have been aligned vertically for easier visualization). These results correspond to the 40,40 SWNT probe imaging the bare Si(100)-OH surface, for a cantilever tip position of -0.5 nm. The images show that the local deformation at the end of the tip is significant, in agreement with the results presented in Table S-1, and that macroscopic deformation is a combination of bending and shearing (shearing occurs because only one corner of the probe contacts the surface).

Figure S-7. Illustration of 40,40 single-wall carbon nanotube probe deformation in the presence of a 16,16 SWNT sample (diameter 2.1 nm). The pictures show that significant local deformation can take place in addition to bending in more than one Cartesian direction simultaneously when the probe is compressed against the sample.

5. References

1. Garcia, R.; Perez, R. *Surf. Sci. Reports* **2002,** *47,* 197.

2. Show, E.S.; Campbell, P.M. and Novak, J.P. *Appl. Phys. Lett.* **2002,** *80,* 2002.

3. Nguyen, C.V.; So, C.; Stevens, R.M.; Li, Y.; Delziet, L.; Sarrazin, P.; Meyyappan, M. *J. Phys. Chem. B* **2004,** *108,* 2816.